Open Archive TOULOUSE Archive Ouverte (OATAO)

OATAO is an open access repository that collects the work of Toulouse researchers and makes it freely available over the web where possible.

Integrated piezoelectric function in a high thermostable thermoplastic PZT/PEEK composite

Delphine Carponcin [a], Eric Dantras [a,*], Lydia Laffont [b], Jany Dandurand [a], Gwenaëlle Aridon [c], Franck Levallois [c], Laurent Cadiergues [d], Colette Lacabanne [a]

[a] Physique des Polymères, Institut Carnot CIRIMAT, Université de Toulouse, 31062 Toulouse, France
[b] MEMO, Institut Carnot CIRIMAT, ENSIACET, 31432 Toulouse, France
[c] EADS Astrium Satellites, 31401 Toulouse, France
[d] Centre National d'Etudes Spatiales, 31401 Toulouse, France

ABSTRACT

A piezoelectric structural material has been developed. Lead Zirconate Titanate (PZT) submicronic nanoparticles have been dispersed in a thermostable high performance thermoplastic polymer Poly(Ether Ether Ketone) i.e. PEEK to ensure piezoelectric properties. The inorganic particles with a mean diameter of 900 nm are polycrystalline as highlighted by HRTEM with a grain diameter estimated at 15 nm. XRD patterns have shown that the crystalline structure is rhombohedral i.e. ferroelectric. The PZT/PEEK composites have been elaborated by extrusion which allows reaching a satisfactory dispersion of particles even at high volume fraction (30% in volume). One of the challenges was to find poling conditions compatible with the thermal stability of the matrix. Indeed, this composite must be poled above the polymer glass transition temperature to improve matching of dielectric permittivity between inorganic and organic phases. The influence of the poling electric field on the final piezoelectric activity of the composite has also been studied to better understand the role of the polymer matrix. Finally, after a poling step, the PZT/PEEK composite exhibits a piezoelectric strain coefficient which can be exploited over a wide temperature range.

1. Introduction

Proposing polymeric based composites with integrated electroactive properties is one of the routes to go further in the development of piezoelectric materials for engineering. Some polymers are intrinsically piezoelectric due to their chemical composition. Poly(vinylidene fluoride) (PVDF) [1], vinylidene fluoride trifluoroethylene (P(VDF–TrFE)) copolymer [2] and P(VDF–TrFE–CFE) terpolymer [3] present good electromechanical coefficient and high ductility. However, their main drawbacks remain the high electric field required to pole them and their poor thermal stability. Organic matrix/inorganic piezoelectric particle composites appear in 1976 [4]. The main interest of the hybrid concept is a required poling field ten times lower than the one of piezoelectric polymers with stable piezoelectric properties until the Curie temperature of the ferroelectric inorganic phase. Later, a wide range of piezoelectric composites was studied. Numerous thermoplastic polymers such as polyethylene [5], polyvinyl chloride [6], polyurethane [7], polymethyl methacrylate [8] and polyamide [9–11] have been employed as matrix and ensure a working temperature until their relatively low melting point. In this work, we propose a piezoelectric composite with a high performance thermostable thermoplastic polymer matrix to enhance the working temperature range of the material. As a result, a structural material with an integrated piezoelectric function is developed. With high thermal transition temperatures, good chemistry stability and high mechanical properties, the PolyArylEtherKetone family gained increased interest due to potential applications in aircraft and spacecraft structures [12,13]. PolyEtherEtherKetone (PEEK) belongs to this family and a lot of work has been devoted to add new functionalities to it. Carbon fibers are largely employed as a mechanical reinforcement in PEEK polymer based composites [14] but other fillers are investigated. The incorporation of carbon nanotubes in a PEEK matrix increases by ten decades the electrical conductivity of the polymer with only few weight percent of fillers [15]. High dielectric permittivity particles may be introduced in PEEK to increase its dielectric properties for microelectronic applications [16]. The common point to these composites is the difficulty of dispersing fillers in the matrix due to its high melting point and quite elevated viscosity. The challenge is then to ensure a satisfactory dispersion of inorganic particles in the polymer matrix. In this way, equivalent electroactive performances are reached for lower filler concentration and polymer mechanical properties tend to be less degraded. Melt mixing is largely used to elaborate thermoplastic based composite. Since PEEK polymer is resistant to most organic solvents, extrusion has been naturally selected as the processing route. Filler dispersion state in the

* Corresponding author: Physique des Polymères, CIRIMAT/Institut Carnot, Université Paul Sabatier, 118 route de Narbonne, 31062 Toulouse Cedex 9, France
E-mail address: eric.dantras@univ-tlse3.fr (E. Dantras).

polymer matrix depends on various extrusion parameters, particularly on the mixing temperature which governs the polymer viscosity [17,18].

One important point regarding piezoelectric composites is the poling step required to develop the piezoelectric property: ceramic particles are ferroelectric and become piezoelectric due to the appearance of a macroscopic polarization. In previous works [19,20], it has been shown that the polarization process is more efficient above the polymer glass transition temperature when the dielectric permittivity of both phases becomes closer. Regarding PEEK matrix, its high glass transition temperature makes the use of a ferroelectric ceramic with a high Curie temperature necessary. Lead Zirconate Titanate (PZT) answers to this need by presenting one of the highest electroactive coefficients in a bulky state and is chosen to bring piezoelectricity to the PEEK matrix.

Here, we report the elaboration and characterization of a piezoelectric PZT/PEEK composite. PZT particles have been chosen submicronically to maintain the mechanical properties of the polymer matrix at a higher volume fraction of inorganic particles [21]. The high Curie temperature of the inorganic phase and high thermal transitions of the organic matrix may be relevant to ensure the piezoelectric property over a wide temperature range. These composites could find some applications in lightweight and high thermal sensors and actuators.

2. Experimental

2.1. Materials

The PEEK polymer used in this study is a commercially semi-crystalline Vestakeep PEEK FP supplied by Evonik Industries AG (Germany) in a 50 μm diameter powder. It is characterized by a glass transition temperature (T_g) of 150 °C and a melting temperature of 340 °C and offers a high degradation temperature with an onset around 580 °C. Ferroelectric Lead Zirconate Titanate (PZT) particles with a mean diameter of 900 nm have been provided by Ferroperm Piezoceramics A/S (Denmark).

2.2. Composite elaboration

The PEEK polymer is of good resistance to most organic solvents, therefore the melting way is the best route to incorporate fillers into this polymeric matrix. Then, ceramic fillers have been dispersed in PEEK by extrusion, an industrial process. For this, a twin-screw extruder (Minilab 2 from Haake) has been used with optimized processing parameters to reach the best particle dispersion. The mixing temperature was 390 °C to ensure a sufficient low viscosity. The mixing time and screw rotation speed were selected following a previous work [17] at 15 min and 30 rpm respectively.

PZT volume fraction has been fixed at 30% in volume since a previous study has shown that mechanical properties of a PA 11/PZT composite stay close to the polymer one until this concentration [22]. After the extrusion step, the composite was hot pressed at 390 °C with the aim to achieve a 200 μm thickness films.

2.3. Analysis techniques

For microstructure observation, a droplet of PZT particle suspension was deposited on commercial copper grids coated with lacey carbon films. Electron transparent samples were obtained.

High-Resolution Electron Microscopy (HRTEM) images were performed using a JEOL JEM 2100F microscope operating at 200 kV and equipped with an Energy Dispersive X-ray (EDX) spectrometer for chemical analysis. The diffraction patterns of the investigated materials are obtained using the Selected Area Electron Diffraction (SAED) mode.

X-ray diffraction (XRD) technique was used to reveal the crystalline structure of PZT particles. The PZT diffractograms were measured using a Rigaku diffractometer with a Cu-Kα (1.54056 Å) radiation source.

Powder XRD pattern was taken in the continuous mode, over a range of 20–60° 2θ with 0.02 degree step size and 5 s dwell per step. For temperature XRD patterns, a powder diffractometer (D8) with carbon filtered Cu-Kα was used. Diffractograms were taken in the continuous mode over a range 43–46 2θ with 0.02 degree step size and 2 s dwell per step every 50 °C from ambient temperature to 500 °C.

A JEOL JSM 6700F Scanning Electron Microscope (SEM) was used to study PZT dispersion in the PEEK matrix. Cryo-cut samples were observed. As PZT density is higher than the PEEK one, backscattered electron detection was used.

A poling procedure is needed for orienting PZT dipoles in order to obtain piezoelectric composites. Composites were poled during 15 min under a static electric field higher than the ceramic coercive field [19]. The influence of two parameters on the poling procedure efficiency was checked: the amplitude of the static electric field and the poling temperature. The electric field was turned off and the samples were short-circuited. Then, the piezoelectric strain coefficient was measured.

Piezoelectric strain coefficient d_{33} was measured 24 h after the poling step, using a PM 200 piezometer supplied by Piezotest (UK), with a strength of 0.25 N at 110 Hz in frequency.

Dynamic Dielectric Spectroscopy (DDS) was performed using a BDS400 within a frequency range from 10^{-1} to 10^6 Hz. The real part ε' of the relative complex permittivity ε^* was measured from −150 to 250 °C with a 5 °C step between each frequency scan.

3. Results and discussion

3.1. PZT microstructure

Fig. 1 depicts the crystal microstructure of PZT particles observed by TEM. Fig. 1(a) reveals particles with an almost spherical shape. The polycrystallinity is highlighted either by the SAED pattern of the PZT particles having a concentric rings and by HRTEM images (Fig. 1(b)) with a grain diameter estimated at 15 nm. The SAED pattern has been indexed by the JCPS card No. 073-222 as rhombohedral crystalline structure.

Furthermore, chemical composition was studied by EDX and has revealed a mean atomic concentration of zirconium at 29%, lead at 49% and titanium at 22% in the PZT formula $Pb[Zr_{0.59}T_{0.41}]O_3$. This composition was found homogeneous in a single particle. Monocrystalline impurities have been also observed and associated to titanium dioxide used in the PZT powder processing.

3.2. PZT crystalline structure

The diffractogram of the as-received PZT powder obtained by XRD is presented in Fig. 2. It is a characteristic of a perovskite crystal structure which is ferroelectric due to its non-centrosymmetry. Around 2θ = 45° (inset pattern), one diffraction peak persists and corresponds to the (202) rhombohedral scattering plane, confirming EDX analysis results. Literature reports that the PZT crystal structure can adopt preferentially two different crystal structures which depend on zirconium and titanium concentrations [23]. For high zirconium concentration, the crystalline structure is rhombohedral; at lower concentration, the structure is tetragonal. However PZT ceramics are commonly used for a specific zirconium/titanium ratio. At the Morphotropic Phase Boundary (MPB), where x = 0.52 in the $Pb[Zr_xTi_{(1-x)}]O_3$ formula, ferroelectric properties reach a maximum due to an increase of the number of allowable dipole poling directions [24,25]. At this particular composition, rhombohedral and tetragonal phases coexist. In our as-received PZT powder, only one ferroelectric crystalline structure coexists which may imply lower ferroelectric properties than usual bulk PZT ones. These observations are explained by a process requiring high energy level used to reduce bulk PZT into submicronic powder leading to some modifications in the chemical stoichiometry.
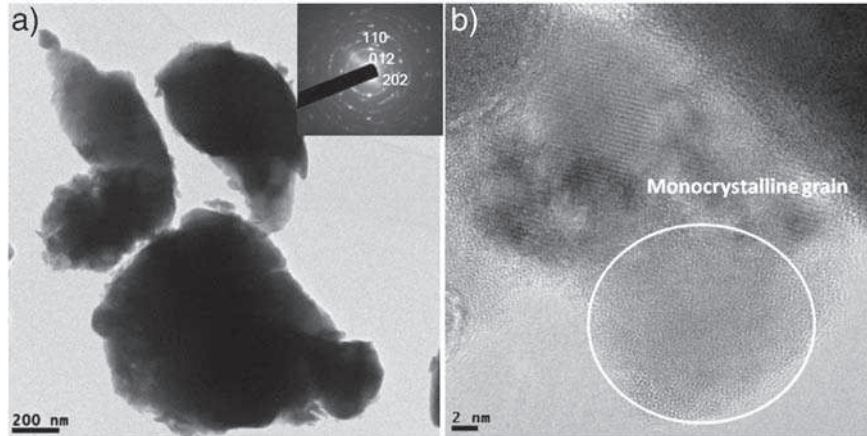
Fig. 1. (a) Bright-field Transmission Electron Microscopy (TEM) image associated with the SAED pattern and (b) High Resolution TEM (HRTEM) of PZT particles.

Two temperature treatments have been selected to promote a crystalline phase coexistence (rhombohedral and tetragonal structures) which is at the origin of the MPB. After 6 h at 790 °C, the diffractogram is slightly modified and the rhombohedral phase is still dominating. A 1100 °C thermal treatment induces the appearance of new diffraction peaks corresponding to the tetragonal phase.

Rhombohedral and tetragonal phases now coexist and will offer highest ferroelectric performances. The aim of this work is to propose a composite with submicronic PZT particles. Consequently, a thermal treatment cannot be used since it leads to the PZT sintering resulting in an increase of PZT particle diameter.

3.3. PZT particle dispersion in PEEK matrix

The dispersion of PZT powder in the thermostable polymeric matrix was studied by SEM in order to check the experimental protocol. Fig. 3 shows a good dispersion of PZT particles in the PEEK matrix. Quasi-spherical particles of PZT are homogeneously dispersed in PEEK. SEM experiments point out that even at high volume fraction of submicronic particles in the matrix, the dispersion is still correct at a nanometric scale.
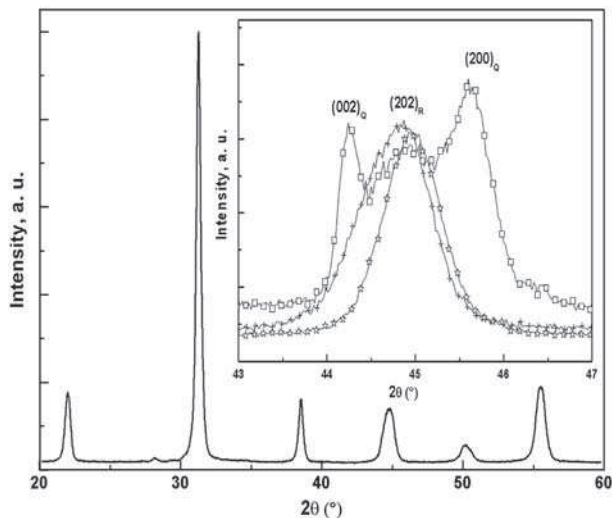
Fig. 2. X-ray diffraction diffractograms of one set of PZT particles measured at room temperature. The inset is a zoom of the peak at $2\theta = 45°$ of PZT particles not heated ($+$), heated at 790 °C ($\star$) and 1100 °C ( ) during 6 h.

3.4. Determination of the PZT Curie temperature

Classic analysis techniques, as differential scanning calorimetry measurements, do not allow pointing out the PZT Curie temperature. Rossetti et al. have demonstrated that the ferro-paraelectric transition of PZT, associated to an endothermic peak of the specific heat capacity, is not observable when zirconium concentration is higher than 35% [26,27].

XRD analysis performed with temperature has been led on PZT powder to estimate the Curie temperature. Three diffractograms, from 43° to 46° 2θ, have been recorded at 200, 300 and 350 °C and compared to the one obtained at room temperature. Fig. 4 shows that the diffraction peak becomes narrow with the heat treatment: the rhombohedral structure is promoted compared to the tetragonal one. At 350 °C, the peak intensity stays close to the one at 300 °C and the maximal amplitude is reached. The PZT crystalline structure is now cubic and corresponds to a paraelectric state. The Curie temperature is comprised between 300 and 350 °C.

3.5. Piezoelectric strain coefficient of PZT/PEEK composite

3.5.1. Influence of the poling temperature
The piezoelectric strain coefficient d_{33} of the PZT/PEEK composite was measured as a function of the poling temperature (Fig. 5). For each temperature, a 10 kV·mm^{-1} electrical field was applied for 15 min in order to make PZT particles piezoelectric. The piezoelectric coefficient was measured 24 h after the poling procedure in order to prevent any dielectric internal stress. For a poling temperature of 230 °C, the d_{33} coefficient reaches a plateau and is equal to 1.7 pC/N. The evolution of the real part of the complex permittivity taken at 1 kHz is also reported as a function of the temperature. At 150 °C, the polymer matrix permittivity, starting from 2.2, begins to increase to reach 2.6 at 210 °C. At these temperatures, the polymer glass transition temperature is reached (T_g of PEEK is around 145 °C) inducing an increase of the molecular mobility. The increased mobility of dipolar groups results in a higher permittivity. This permittivity value has a direct impact on the piezoelectric strain coefficient. As the polymer permittivity increases, the polarization of PZT particles embedded in the polymer matrix is higher; consequently, the composite piezoelectric strain coefficient increases. During the poling process, a better impedance matching between the inorganic and organic phases is reached. Above 220 °C, two phenomena act resulting in a compromise. The polymer dielectric permittivity keeps on increasing due to the appearance of conductivity at elevated temperature. Therefore, at the same time, temperature is getting closer to the PZT Curie temperature which explains that, from a global point of view, ferroelectric properties decrease [19].
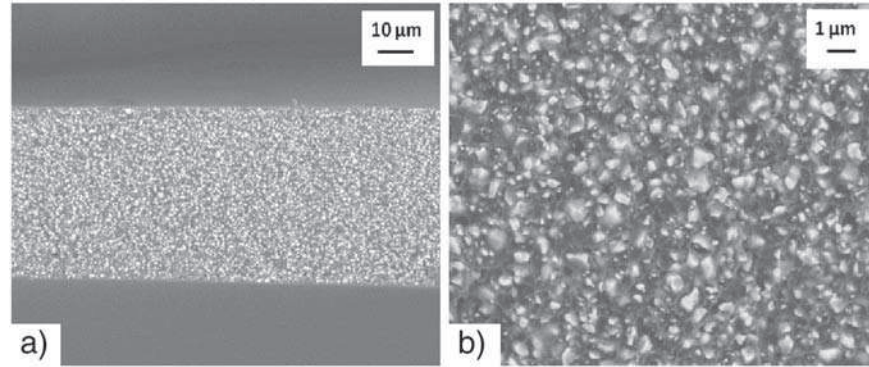
Fig. 3. Scanning Electron Microscopy (SEM) image of a PZT/PEEK composite loaded at 30% in volume for a magnification of (a) ×1000 and (b) ×5000.

A piezoelectric activity sets up when the poling temperature is higher than 160 °C which corresponds to 10 °C above the glass transition temperature of PEEK matrix. This result is in total agreement with the literature [10,28,29] since piezoelectric composites with a polymeric matrix must be poled above their glass transition temperature in order to observe a macroscopic electroactive behavior.

3.5.2. Influence of the poling electric field amplitude

The piezoelectric strain coefficient d_{33} of the PZT/PEEK composite was studied as a function of the poling electric field amplitude (Fig. 6). For each electric field value, the temperature is set at 230 °C and the electric field is applied during 15 min. The piezoelectric strain coefficient becomes quite stable (around 2 pC/N) above 10 kV/mm showing that a saturation effect acts in the dipolar orientation of the inorganic fillers. The piezoelectric activity reported here is small compared to literature data. One explanation is the PZT powder crystalline structure. It has been demonstrated that this last is compatible with a ferroelectric state but does not belong to the Morphotropic Phase Boundary where the ferroelectric properties are the most important. Furthermore, this originality of this work is to deal with submicronic PZT particles. The submicronic characteristic may induce a decrease of cooperativity in particle dipole orientation in the establishment of the piezoelectric property. At a macroscopic scale, it acts on piezoelectric activity efficiency.

Other explanation takes into account the influence of the polymer matrix nature. The piezoelectric activity of PZT/PEEK composite has been compared to the PZT/Polyamide 11 (PA 11) composite one. The PZT/PA 11 composite has been elaborated in the exact same conditions
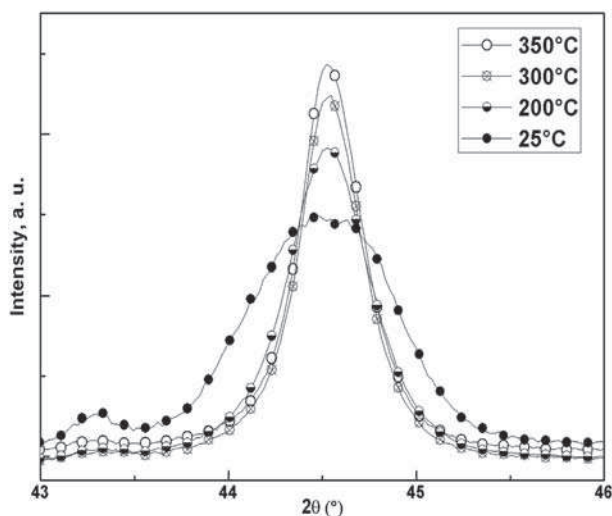
than the PZT/PEEK composite with the exception of the extrusion temperature which was fixed at 210 °C. The composite is also loaded at 30% in volume with the same 900 nm diameter PZT powder. Regarding poling procedure, only the temperature is different: 80 °C instead of 230 °C but always above the glass transition of the polymer matrix. For poling field above 10 kV/mm, a 30% increase of the d_{33} coefficient (from 2 to 2.6 pC/N) between both composites is observed confirming that the polymer matrix nature plays a major role in the piezoelectric activity in organic/inorganic piezoelectric composite.

3.5.3. Influence of the polymer dielectric permittivity

One of the physical parameters of the polymer matrix which may justify the evolution of the piezoelectric strain coefficient between PZT/PA 11 and PZT/PEEK composites is the dielectric permittivity. Fig. 7 points out the evolution of the real part of the dielectric permittivity taken at 1 kHz of neat PA 11 and neat PEEK as a function of temperature. It appears that the dielectric permittivity step at the polymer glass transition temperature is more pronounced for polyamide 11 than for PEEK. This results in a higher ε value at the poling temperature of PZT/PA 11 composite ($\varepsilon_{PA\ 11\ at\ 80\ °C}$ = 3.9) than at the poling temperature of PZT/PEEK composite ($\varepsilon_{PEEK\ at\ 230\ °C}$ = 2.7), corresponding to a 44% increase in the permittivity value.

Fig. 4. X-ray diffraction spectra of PZT particles measured at room temperature, 200, 300 and 350 °C.
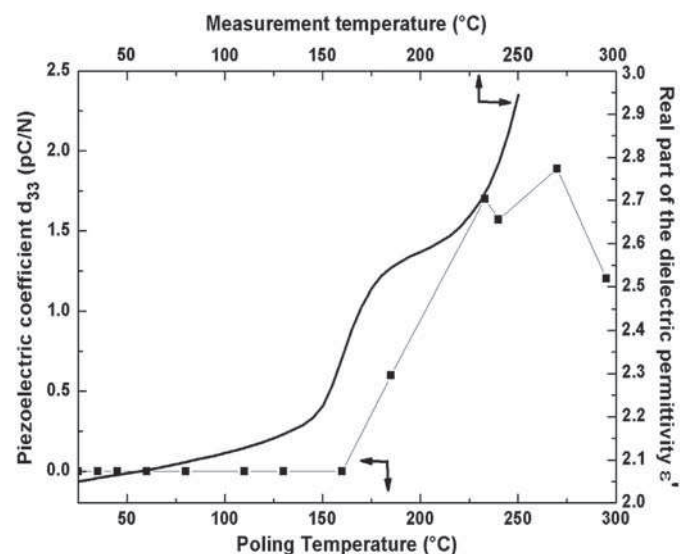

Fig. 5. Influence of the poling temperature on the piezoelectric strain coefficient d_{33} (squares) measured at room temperature for a PZT/PEEK composite loaded at 30% in volume. Real part of the complex dielectric permittivity (taken at 1 kHz) of the PEEK matrix (solid line) is reported as a function of temperature.
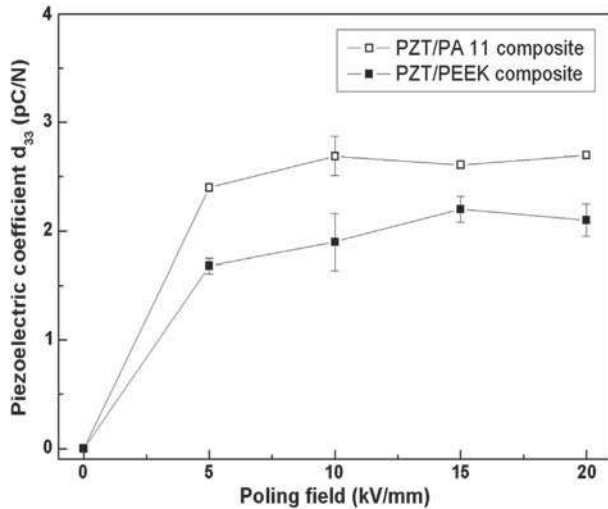
Fig. 6. Influence of the poling electric field amplitude on the piezoelectric strain coefficient d_{33} measured at room temperature for a PZT/PEEK composite (filled squares) and PZT/PA 11 composite (empty squares) both elaborated by extrusion and loaded at 30% in volume.

The local electric field E_c really seen by the ferroelectric PZT particles is given by [30]:

$$\vec{E}_c = \frac{3\varepsilon_1}{\varepsilon_2 + 2\varepsilon_1} \vec{E}_0 \qquad (1)$$

where E_0 is the electric field applied to the composite, and ε_1 and ε_2 the dielectric permittivity of the organic and inorganic phases respectively. This equation shows that the electric field acting on the ceramic particle in a polymer matrix is controlled by the dielectric constant of the polymer matrix. Enhancing this last parameter will improve the efficiency of the piezoelectric ceramic poling.

The same 900 nm diameter PZT particles have been dispersed at 30% in volume in a high permittivity polymer, the P(VDF–TrFE–CFE) with $\varepsilon' = 17.3$. This composite has been poled at 5 kV/mm during 15 min at 80 °C. The d_{33} coefficient of the PZT/P(VDF–TrFE–CFE) composite reaches 16.2 pC/N compared to 2.4 pC/N for PZT/PA 11 composite and 1.7 pC/N for PZT/PEEK composite. These values corroborate that the piezoelectric activity of inorganic/organic composites is tunable with the dielectric properties of the organic phase.
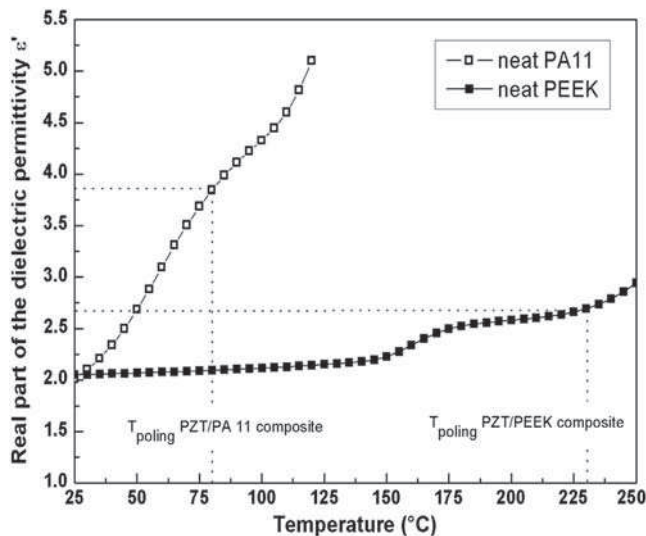

Fig. 7. Evolution of the real part of the complex dielectric permittivity (taken at 1 kHz) as a function of temperature for neat PEEK polymer matrix (filled squares) and PA 11 polymer matrix (empty squares).

4. Conclusion

Lead Zirconate Titanate (PZT) submicronic particles were dispersed in a high performance thermostable polymer matrix to elaborate a new electroactive structural composite. The XRD study of these ceramic particles exhibits a rhombohedral crystalline structure which presents ferroelectric properties. It is important to note that the PZT structure of submicronic particles does not belong to the Morphotropic Phase Boundary (MPB) where PZT ceramics are employed most of the time in industrial applications. This rhombohedral crystalline structure is inherent to the high energetic milling process applied on the bulk ceramic for realizing submicronic morphologies.

Films of electroactive polymer based composite have been elaborated by extrusion. We have shown the ability of this industrial process to disperse particles into a polymer with rigid chains.

Ferroelectric particles need to be poled to ensure piezoelectric function. This step has been realized once PZT/PEEK composites are achieved. The polymer matrix plays an important role in this step. A piezoelectric coefficient appears i.e. the PZT/PEEK composite becomes electroactive only when the poling field is applied above the polymer glass transition temperature. At this temperature, polymer mobility begins to increase as well as polymer permittivity. By this way, the poling electric field is more efficient and PZT particles, as well as PZT/PEEK composite, acquire a piezoelectric activity. The same PZT particles have been dispersed not only in a PA 11 matrix but also in a high permittivity P(VDF–TrFE–CFE) matrix. The evolution of the piezoelectric strain coefficient as a function of the employed polymer matrix has shown the influence of the dielectric permittivity value of the organic phase.

The performances reached by the PZT/PEEK composite open new horizons for designing lightweight smart structural materials with an integrated actuation or transduction property requiring high thermal stability.

References

[1] L. Ibos, A. Bernes, C. Lacabanne, Ferroelectrics 320 (2005) 483.
[2] G. Teyssedre, C. Lacabanne, Ferroelectrics 171 (1995) 125.
[3] B. Chu, X. Zhou, B. Neese, Q.M. Zhang, F. Bauer, Ferroelectrics 331 (2006) 35.
[4] T. Furukawa, K. Fujino, E. Fukada, Jpn. J. Appl. Phys. 15 (1976) 2119.
[5] T. Furukawa, K. Ishida, E. Fukada, J. Appl. Phys. 50 (1979) 4904.
[6] L. Liu, J.C. Grunlan, Adv. Funct. Mater. 17 (2007) 2343.
[7] K.A. Hanner, A. Safari, R.E. Newham, J. Runt, Ferroelectrics 100 (1989) 255.
[8] G. Chen, Y. Li, H. Shimizu, Carbon 45 (2007) 2334.
[9] J. Capsal, E. Dantras, J. Dandurand, C. Lacabanne, J. Non-Cryst. Solids 353 (2007) 4437.
[10] K. Li, H. Wang, A. Ding, Polym. Sci. 52 (2010) 438.
[11] I. Babu, D.A.V.D. Ende, G.D. With, J. Phys. D. Appl. Phys. 43 (2010) 425402.
[12] J.C. Seferis, Polym. Compos. 7 (1986) 158.
[13] I. Chang, SAMPE Q. 19 (1988) 29.
[14] C. Soutis, Mater. Sci. Eng. A 412 (2005) 171.
[15] A. Diez-Pascual, M. Naffakh, M.A. Gomez, C. Marco, G. Ellis, M.T. Martinez, A. Anson, J.M. Gonzales-Dominguez, Y. Martinez-Rubi, B. Simard, Carbon 47 (2009) 3079.
[16] V.S. Nisa, S. Rajesh, K.P. Murali, V. Priyadarsini, S.N. Potty, R. Ratheesh, Compos. Sci. Technol. 68 (2008) 106.
[17] D. Carponcin, E. Dantras, G. Aridon, F. Levallois, L. Cadiergues, C. Lacabanne, Compos. Sci. Technol. 72 (2012) 515.
[18] B. Krause, P. Pötschke, L. Häubler, Compos. Sci. Technol. 69 (2009) 1505.
[19] T.M. Kamel, F.X.N.M. Kools, G.D. With, J. Eur. Ceram. Soc. 27 (2007) 2471.
[20] J. Capsal, E. Dantras, L. Laffont, J. Dandurand, C. Lacabanne, J. Non-Cryst. Solids 356 (2009) 629.
[21] J. Capsal, C. Pousserot, E. Dantras, J. Dandurand, C. Lacabanne, Polymer 51 (2010) 5207.
[22] D. Carponcin, E. Dantras, J. Dandurand, C. Lacabanne, L. Laffont, L. Cadiergues, G. Aridon, F. Levallois, 53rd AIAA/ASME/ASCE/AHS/ASC Structures, Structural Dynamics and Materials Conference Honolulu-USA, 2012.
[23] B. Jaffe, R.S. Roth, S. Marzullo, J. Appl. Phys. 25 (1954) 809.
[24] M.R. Soares, A.M.R. Senos, P.Q. Mantas, J. Eur. Ceram. Soc. 19 (1998) 1865.
[25] M.R. Soares, A.M.R. Senos, P.Q. Mantas, J. Eur. Ceram. Soc. 20 (2000) 321.
[26] G.A. Rossetti, P.H. Cahill, R.R. Biederman, A. Sacco, Mater. Lett. 41 (1999) 72.
[27] G.A. Rossetti, A. Navrotsky, J. Solid State Chem. 144 (1999) 188.
[28] C. David, J. Capsal, L. Laffont, E. Dantras, C. Lacabanne, J. Phys. D. Appl. Phys. 45 (2012) 415305.
[29] X. Liu, C. Xiong, H. Sun, L. Dong, R. Li, Y. Liu, Mater. Sci. Eng. B 127 (2006) 261.